

Architecture of the SARS coronavirus prefusion spike

Daniel R Beniac¹, Anton Andonov^{1,2}, Elsie Grudski¹ & Tim F Booth^{1,2}

The emergence in 2003 of a new coronavirus (CoV) responsible for the atypical pneumonia termed severe acute respiratory syndrome (SARS) was a stark reminder that hitherto unknown viruses have the potential to cross species barriers to become new human pathogens. Here we describe the SARS-CoV 'spike' structure determined by single-particle cryo-EM, along with the docked atomic structures of the receptor-binding domain and prefusion core.

The surface protein, or 'spike,' of enveloped viruses is an essential component for infection of the host cell, responsible for both binding to cellular receptors and subsequent fusion of viral and cellular membranes. Cell attachment and entry are crucial functions affecting the host range and cell tropism of viral infections. Fusion is achieved through conformational changes in the fusion core of the spike molecule¹, allowing entry of viral nucleocapsids into the host cell to initiate replication. Coronaviruses commonly cause relatively mild respiratory infections in humans², and their spike protein gives these viruses their distinctive crown-like appearance³. Coronavirus spikes are trimeric globular proteins approximately 150 Å in diameter and are attached to the virion envelope by a narrow stalk (Fig. 1). In SARS-CoV, the spike has a mass of about 500 kDa³, making it the largest type 1 viral fusion spike protein^{4,5}. Only a small part (18%) of the prefusion SARS-CoV spike structure, including the fusion core⁶ and receptor-binding domain⁷, has hitherto been solved to atomic resolution. The fusion core of SARS-CoV consists of two heptad-repeat regions and is highly similar to those of other coronaviruses⁸ and to other type 1 fusion proteins, such as hemagglutinin (HA) from influenza⁵, gp41 from human immunodeficiency virus⁴ and the fusion protein of paramyxovirus⁹. The entire spike gene is highly conserved across all three main coronavirus groups, suggesting that these groups are specialized for a common mode of attachment in addition to sharing a similar fusion mechanism with other type 1 fusion proteins⁸. We set out to delineate the complete SARS-CoV spike structure, using cryo-EM and molecular docking to determine the positions of the fusion core and receptor-binding domains.

For structural investigations, we inoculated Vero E6 cells with SARS-CoV, purified virus particles from the supernatant using an iodoxanol density gradient (Supplementary Methods and Supplementary Fig. 1 online) and analyzed intact virion preparations by

cryo-EM (Fig. 1) and three-dimensional image processing (Supplementary Figs. 2 and 3 online). To ensure biological safety, specimens were γ -irradiated and viral inactivation was verified. The irradiation dose used (2 Mrad) caused no obvious changes in virion structure, and we observed no radiolysis of viral proteins in SDS-PAGE results. Moreover, antigenicity to both patient sera and monoclonal antibodies was retained, as measured by ELISA and western blotting (Supplementary Fig. 1), indicating that epitopes were structurally intact. Radiation effects are random, so no structural changes were expected to appear after image averaging. Although SARS-CoV virions appear to be pleomorphic in negative-staining images, they are much more regular in shape when observed by cryo-EM (Fig. 1).

Virions average 1,185 Å in diameter, including the spikes, with a 36-Å-thick lipid bilayer envelope that is approximately spherical and has an average diameter of 865 Å (Fig. 1). Most are rounded and are

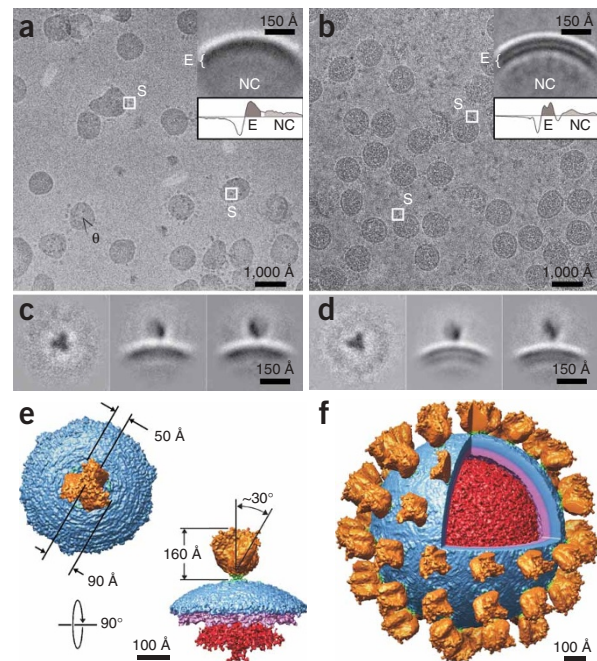


Figure 1 Cryo-EM and three-dimensional reconstruction of SARS-CoV. (a,b) Images at 8 μ (a) and 5.5 μ (b) defocus. S indicates spikes; arrowhead marks angle (θ) measured between two spikes. Inset shows envelope (E) and nucleocapsid (NC). (c,d) Select two-dimensional class averages from the defocus data in a and b, respectively. (e) Spike attached to the viral envelope by a narrow stalk. (f) Model of SARS-CoV with spikes spaced isotropically at 23.8°, surface-sectioned to reveal the interior. Orange, spike; green, stalk; blue and pink, envelope bilayer; red, nucleocapsid.

¹Viral Diseases Division, National Microbiology Laboratory, Public Health Agency of Canada, 1015 Arlington Street, Winnipeg, Manitoba, R3E 3R2, Canada.

²Department of Medical Microbiology, University of Manitoba, Winnipeg, Manitoba, R3E 0W3, Canada. Correspondence should be addressed to T.F.B. (tim_booth@phac-aspc.gc.ca).

Received 17 March; accepted 23 June; published online 16 July 2006; doi:10.1038/nsmb1123

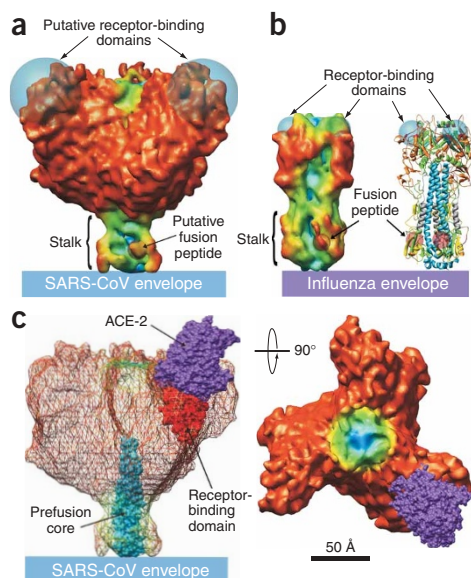


Figure 2 Fitting atomic-resolution structures within the spike. (a,b) Putative locations of the fusion peptide and receptor-binding domain in the SARS spike (a) and influenza HA (b; PDB entry 1HA0)¹⁰, shown at the same resolution, colored according to cylindrical depth. (c) The SARS spike in side and end-on views, with the docked heptad-repeat prefusion core (PDB entry 2FXP⁶) and receptor-binding domain (PDB entry 2AJF⁷) bound to ACE-2.

readily observed in the frozen-hydrated state, although some virions are oval or kidney-shaped. Individual spikes can be seen from both the side-view and end-on perspectives (Fig. 1a–d). Images of spherical virus ($n = 140$) were selected, aligned and circularly averaged (Fig. 1), giving a maximum average diameter of 864 ± 44 Å, with a gap of about 40 Å between the envelope and nucleocapsid (Fig. 1a,b). The inner core or nucleocapsid is a density inside the lipid envelope with radius of approximately 320 Å (Fig. 1a–d). Image processing showed that the spike has three distinct lobes visible in end-on view, with a triangular shape projecting 160 Å above the viral envelope (Fig. 1e), confirming that it is trimeric.

A three-dimensional reconstruction of the spike of SARS-CoV (Fig. 1e) was generated using projection matching of 8,386 individual spike images taken at a range of defocus values from 3.3 to 12.7 μ. The envelope-anchored spike has a structure about 180 Å in diameter, with three distinct protuberances or domains 50 Å thick on each subunit of the trimer (similar in appearance to the blades of a propeller) and a thin stalk connecting the spike to the viral envelope. The ‘blades’ are twisted at an angle of $\sim 30^\circ$ to the axis of symmetry and are almost certainly composed of the S1 domain of the SARS-CoV S polypeptide (Supplementary Fig. 4 online).

Although the α -helices of the HR2 fusion core domain cannot be identified at 16-Å resolution (estimated by Fourier shell correlation, Supplementary Fig. 3), we were able to dock the HR2 structure⁶ within the trimer using SITUS (correlation coefficient = 0.966; Fig. 2 and Supplementary Fig. 4). The location of the domain is constrained, in that it must form the stalk of the spike and the base must contain the transmembrane region to attach to the virion envelope. The fusion core must also extend distally away from the virion envelope and be centered on the three-fold axis of symmetry. For comparison, prefusion HA from influenza (PDB entry 1HA0)¹⁰ is shown at the same resolution (Fig. 2b). The stalks of both structures are similar in size and shape (Fig. 2a,b), containing a deep groove (green) and helical left-handed struts on the vertices (orange). Both stalks have a distinct lobe on one

side of the groove (the right side in Fig. 2) that corresponds to the uncleaved fusion peptide in the influenza structure.

Two cell-surface molecules, ACE-2 and CD209, have been shown to act as receptors for the SARS-CoV spike protein^{7,11}. Using SITUS, we docked the spike protein’s ACE-2 receptor-binding domain structure within the spike at the distal end (Fig. 2 and Supplementary Fig. 4), with a high correlation score of 0.891. This location for the ACE-2-binding region on the SARS spike is consistent with a cell surface-binding function and is equivalent to the receptor-binding domain of influenza HA, which is also at the distal end of the molecule. The average angle between each spike, from 145 angle measurements, is $23.8^\circ \pm 9.7^\circ$ (Fig. 1a). This gives an average of 65 trimeric spikes per virus particle (Fig. 1f), assuming even spacing on a spherical surface 865 Å in diameter. This is close to the 66.7 trimeric spikes per virion that has been predicted by biochemical studies¹². Larger virions, with an envelope diameter of 1,000 Å, are estimated to have about 100 spikes. Three different models of the virus with icosahedral distributions of 60 spikes were tested by projection matching against a subset of the data containing the 140 roundest images. In all three cases, the spikes were blurred in the reconstruction, indicating a nonicosahedral distribution or a virion surface that is too irregular to reveal symmetry. Our findings demonstrate that the SARS-CoV has an envelope with an inner protein core shell (Fig. 1) enclosing a volume of lower density, consistent with an RNA content. Immunogold labeling of disrupted virions resulted in labeled nucleocapsid protein on this internal layer (Supplementary Fig. 1).

The envelope of SARS-CoV contains very large club-shaped spikes. This may be a functional adaptation allowing multiple receptor specificities for large, 45- to 90-kDa molecules. Mutations in the spike gene are correlated with altered pathogenesis and virulence in other coronaviruses^{13,14}. Thus, the coronavirus spike structure may confer redundancy that enhances host range and viral evolution. Defining the structure and receptor-binding domain of the coronavirus spike may facilitate development of both vaccines and antiviral compounds specific for this family of viruses.

Note: Supplementary information is available on the Nature Structural & Molecular Biology website.

ACKNOWLEDGMENTS

This work was partly funded by grants from the Office of the Chief Scientist, Health Canada.

COMPETING INTERESTS STATEMENT

The authors declare that they have no competing financial interests.

Published online at <http://nature.com/nsmb/>

Reprints and permissions information is available online at <http://npg.nature.com/reprintsandpermissions/>

- Earp, L.J., Delos, S.E., Park, H.E. & White, J.M. *Curr. Top. Microbiol. Immunol.* **285**, 25–66 (2005).
- Weiss, S.R. & Navas-Martin, S. *Microbiol. Mol. Biol. Rev.* **69**, 635–664 (2005).
- Song, H.C. *et al. J. Virol.* **78**, 10328–10335 (2004).
- Weissenhorn, W., Dessen, A., Harrison, S.C., Skehel, J.J. & Wiley, D.C. *Nature* **387**, 426–430 (1997).
- Skehel, J.J. & Wiley, D.C. *Annu. Rev. Biochem.* **69**, 531–569 (2000).
- Hakansson-McReynolds, S., Jiang, S., Rong, L. & Caffrey, M. *J. Biol. Chem.* **281**, 11965–11971 (2006).
- Li, F., Li, W., Farzan, M. & Harrison, S.C. *Science* **309**, 1864–1868 (2005).
- Xu, Y. *et al. J. Biol. Chem.* **279**, 30514–30522 (2004).
- Chen, L. *et al. Structure* **9**, 255–266 (2001).
- Chen, J. *et al. Cell* **95**, 409–417 (1998).
- Jeffers, S.A. *et al. Proc. Natl. Acad. Sci. USA* **101**, 15748–15753 (2004).
- Guillen, J., Perez-Berna, A.J., Moreno, M.R. & Villalain, J. *J. Virol.* **79**, 1743–1752 (2005).
- de Haan, C.A. *et al. J. Virol.* **79**, 14451–14456 (2005).
- Baric, R.S., Yount, B., Hensley, L., Peel, S.A. & Chen, W. *J. Virol.* **71**, 1946–1955 (1997).